

Lunar Ascent of the Apollo 17 in Television Broadcast

Julius A. Birch

(Dated: March 16, 2018)

We analyze the Apollo 17 ascent from the lunar surface that occurred on December 14, 1972. The lunar ascent was captured by a remotely operated pan-zoom-tilt (PZT) camera on the Lunar Roving Vehicle parked some distance away, and broadcasted on television to the audiences on Earth. We use known features of the camera PZT to extract the angle above the horizon (elevation) as a function of time of the craft in the TV broadcast. We then compare the craft's reconstructed trajectory to that of the Apollo 11 Lunar Module Ascent Stage. We list the differences in Vertical Rise and early Orbit Insertion phases, and what makes them anomalous.

Contents

1. Introduction	3
2. Tracking the Lunar Ascent	4
2.1. The Frames	5
2.2. The PTZ Drive and Movements of the Camera	5
2.3. Trajectory Reconstruction	6
2.4. The Scene	12
3. The Apollo Lunar Ascent Trajectory	14
3.1. Apollo 11 Data	15
4. Vertical Rise and Early Orbit Insertion Phase of the Craft in TV Broadcast	17
5. Discussion and Conclusions	20
References	23

1. INTRODUCTION

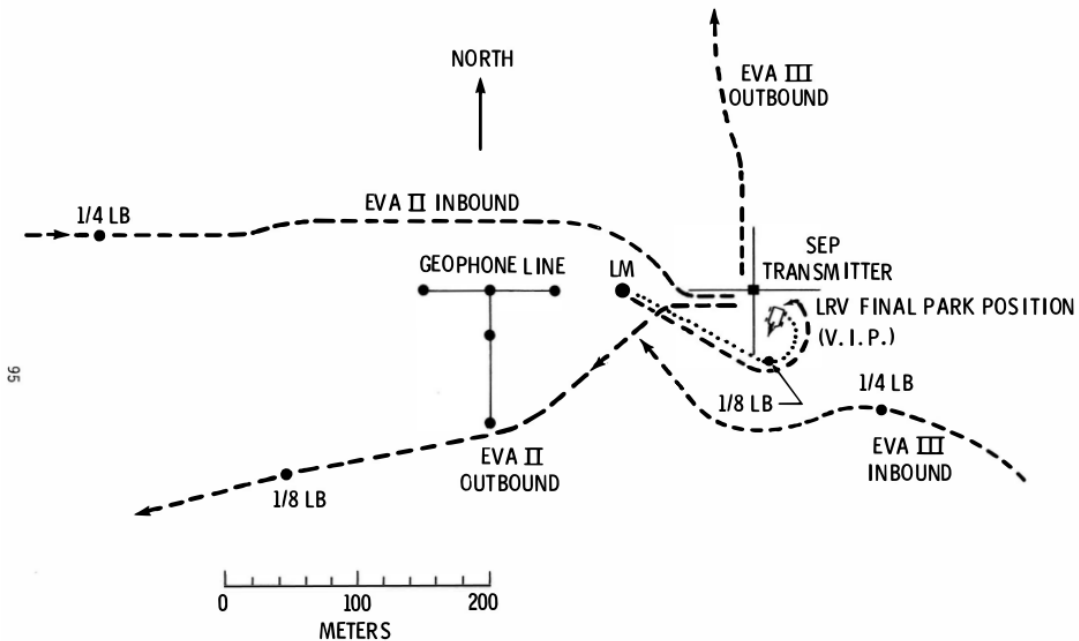


FIG. 1: The January 1972-map of the Apollo 17 landing site on the Moon shows the planned final parking position of the Lunar Roving Vehicle (LRV) carrying the camera that would broadcast the ascent in December of the same year. [1]

According to official NASA documents, Apollo 17 was the final mission of the Apollo program. It was launched on December 7, 1972, at 12:33 Eastern Standard Time (EST). The mission was reported to have landed in the Taurus Littrow valley and over three day stay on the lunar surface have completed three moon-walks, taking lunar samples and deploying scientific instruments. For extended mobility a Lunar Roving Vehicle (LRV) was brought along. The crew returned to Earth on December 19, 1972, after a 12-day mission. [2]

It was reported that the Apollo 17 Lunar Module (LM) Ascent Stage (AS) took off from the lunar surface on December 14, 1972, at 17:55 EST. The ascent was tracked by a camera on the LRV parked some distance away, as shown on the map of the landing site in Fig. 1. The TV camera was controlled remotely by NASA camera operator Ed Fendell, who somehow managed to continuously track the LM AS for the first 29 seconds of ascent. To this day, this is considered to be one of the best video recordings from the entire Apollo program.

The purpose of this report is to reconstruct the lunar ascent of the craft in the television broadcast [3] in terms of the craft's elevation as a function of time, and then to extract the parameters of the craft's propulsion. In Sec. 2 we reconstruct how the camera tracked the craft's ascent. We base

the reconstruction on the analysis of discontinuities in the recorded motion using the fact that the physical trajectory was of the continuity class $C(1)$, that is, continuous in position and velocity. In Sec. 3 for comparison we extract the features of the Apollo 11 lunar ascent, namely, the duration of the Vertical Rise phase, the moment of pitch-over, and the subsequent pitch-adjustment that comprise the early Orbit Insertion phase. In Sec. 4 we do the same for the craft in the TV broadcast. In Sec. 5 we discuss the two trajectories and present our conclusions.

2. TRACKING THE LUNAR ASCENT

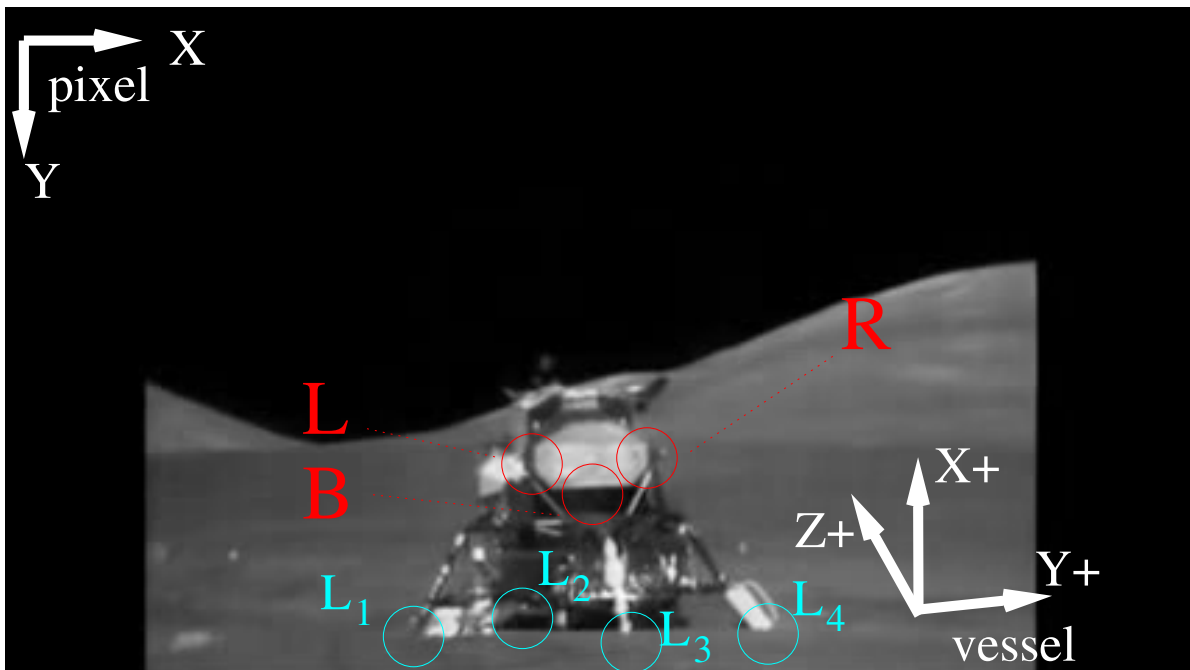


FIG. 2: The three points (L,R and B) on the crew compartment of the LM ascent stage were used to find the attitude and azimuth in the frame -00:00.2. Also shown are the four landing gear feet ($L_{1..4}$) which were used to determine scene angles, and the two coordinate systems used in assessing the motion, that of the principal axes of the camera, and that of the LM.

In this section we find the elevation of the craft in the TV television broadcast [3] as a function of time.

The section is organized as follows. First, we describe the camera based on the available documentation. This allows us to extract the raw tracking information, in which the craft vertical position is given in terms of the relative attitude in the maximal field-of-view (FOV).

Then, we isolate the jump discontinuities from the relative attitude as a function of time, which we

associate with either change in tilt rate, or to a switch from zoom-out to zoom-in. We show how in the process we are also able to extract the zoom as a function of time.

2.1. The Frames

At the time of writing of this report there were a number of video clips of the Apollo 17 LM ascent available on-line [3] They are all of similar fairly high quality, and are much longer than the liftoff itself.

The camera employed a so called Field-sequential Color System (FSCS) [4], in which single color fields are collected through a rotating red, green and blue filter. To reduce transmission bandwidth, the camera was modified from original specifications to broadcast single color fields at 30 fps. On Earth, three consecutive fields would be assembled in a single color frame at the same 30 fps rate. [5, 6] For that reason we extract the individual frames at the rate $r = 10$ fps, so the frames are 0.1 second apart. From video clips the individual frames were extracted in JPEG format using the tool `ffmpeg`. [7] Their pixel values comprise four channels (RGBA) 8-bit deep. From each JPEG we extracted red channel, and created new monochromatic JPEG image in which all color channels were identical to red.

Finally, we set as the zero-time the exact moment of liftoff, and report all frames and their times with respect to it.

2.2. The PTZ Drive and Movements of the Camera

The following can be said about the PTZ camera that tracked the craft in the television broadcast [3]:

- Its tilt rate was reported to be fixed at the values $\omega = 0, \pm 3^\circ/\text{s}$, and its zoom was in the range 6:1 to 1:1, that is, from the focal length of $f = 75$ mm and horizontal (vertical) field-of-view (FOV) of 9° (7°), to $f = 12.5$ mm and FOV of 54° (42°). [8]
- Its zoom was motorized, and the inspection of the footage, e.g., the frames 01:56.4 through 02:10.1 in [3], yields $\Delta t_Z = 13.7$ s as the time it takes the zoom to go from one extremum to the other.

From the inspection of the footage [3] the following can be said about PTZ movements of the camera:

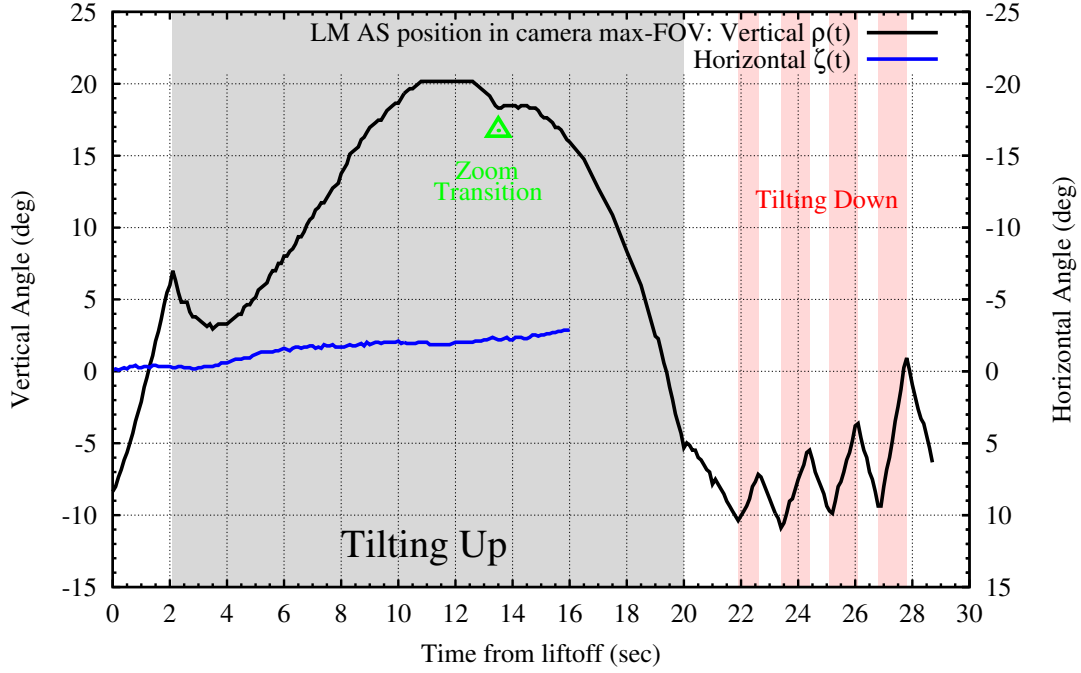


FIG. 3: The relative elevation ρ (in black) and the azimuth ζ (in blue) of the LM AS in the camera FOV(1:1), and the camera movements (tilt up, in gray; tilt down in red; zoom transition at green point) revealed by the jump discontinuities in $\dot{\rho}$.

- Prior to liftoff the camera zoomed in on the LM AS, and at the time $t = -0.2$ s it starts to zoom-out. Upon reaching the maximal zoom-out it reverses the direction of zoom and then starts to zoom-in. Once it reaches the maximal zoom-in the zoom no longer operates.
- Soon after liftoff the camera tilts up to follow the LM AS. At some point the tilt up stops. Later the camera performs four short tilt-downs.
- The camera maintains continuous view of the LM AS concluding with the frame 00:28.7 s after which the LM AS leaves the FOV across the left edge. The camera then starts to wander to the left and sometime later catches with the LM AS.

2.3. Trajectory Reconstruction

Trajectory reconstruction is a standard problem when tracking objects by the camera, e.g., cf. [9] and references therein.

Firstly, we determine relative elevation $\rho = \rho(t)$ and azimuth $\zeta = \zeta(t)$ of the craft in the camera FOV. For that purpose we use three points, which we call, the point B , and the points L and R . Their location on the LM AS crew compartment is shown in Fig. 2. We track these points from

the frames -00:00.2 to 00:28.7. For the conversion of their pixel value to the relative angles in the camera FOV we use pin-hole model of the camera, and assume maximal FOV. The pin-hole model suffices considering that the anticipated distances between the camera and the craft are much greater than the focal length. Moreover, we calculate angular distances in the frames from their average scales. That is, we do not use $\tan \rho = y/f = Y/Z$, where Y, Z are the positions of the object in space while y its projection onto camera plane and f the focal length. Rather, we use $\rho = \sigma \cdot \Delta p_y$, where the average scale $\sigma = \text{VFOV}/\Pi_y$ is the ratio of vertical FOV to the number of pixels in the y -direction Π_y , while $\Delta p_y \in [-\Pi_y/2, \Pi_y/2]$ is the distance in pixels of the object from the center of frame. As is common knowledge, in doing so we make a systematic error in ρ of

$$\varepsilon_\rho = \arctan\left(\frac{2\Delta p_y}{\Pi_y} \tan \frac{\text{VFOV}}{2}\right) - \sigma \cdot \Delta p_y, \quad (2.1)$$

which achieves absolute maximum near the top and bottom middle of the half frame, and which for $\text{VFOV}=42^\circ$ is less than 1% (0.4°) in magnitude. In Fig. 3 we report relative elevation ρ and azimuth ζ found this way.

Obviously, we may assume that the camera is uncalibrated so a question arises whether the radial distortion is relevant. [10] We notice that for the first 13 s the craft is either near the center of the frame, or near one of the principal (mostly y -) axis. In addition, the scene depicted in the frames was captured by one of the Hasselblad photographic cameras with its nearly distortion-free Zeiss Biogon 60mm/f5.6 lens. [11] Qualitative comparison between the photographs and the frames suggests the radial distortion in the camera not to be significant.

In the absence of panning, the assumptions above allow us to use linear model for the absolute elevation η and azimuth α given by,

$$\eta = \mu + \Phi \cdot \rho, \quad (2.2)$$

and

$$\alpha = \Phi \cdot \zeta. \quad (2.3)$$

Here, $\Phi = \Phi(t)$ is the ratio of the FOV at time t to $\text{FOV}(1:1)$,

$$\Phi(t) = \frac{\text{HFOV}(t)}{\text{HFOV}(1:1)} = \frac{\text{VFOV}(t)}{\text{VFOV}(1:1)}. \quad (2.4)$$

We now posit that the motion of the craft in the television broadcast [3] is of continuity class $C(1)$. This then means that the functions $\eta = \eta(t)$ and $\alpha = \alpha(t)$ are $C(1)$, too. In particular, at

any apparent discontinuity of ρ at time instance t^* it has to be that the left and the right limit of $\dot{\eta} = d\eta/dt$ are equal, $\dot{\eta}^L(t) = \dot{\eta}^R(t), \forall t \geq 0$.

From the video clip it transpires that when the camera zoom was engaged it went from one extremum to the other and did not stop or change direction mid-way. Considering that the zoom was driven by an electric motor rotating at a constant rate which direction could be changed, it transpires that the zoom-in (Φ^+) and the zoom-out (Φ^-) functions are reverse of each other. This we write as,

$$\Phi^+(t) = \Phi^-(\Delta t_Z - t), \quad (2.5)$$

where $\Delta t_Z = 13.7$ s is known.

Inspection of ρ in Fig. 3 suggests that $\dot{\rho}(t)$ has a number of jump-discontinuities. We isolate time instances when the jump-discontinuities occur in the first column of Tbl. I. Let t_i be an instance when $\dot{\rho}_i = \dot{\rho}(t_i)$ is discontinuous, meaning that the left $\dot{\rho}_i^L$ and the right $\dot{\rho}_i^R$ limits differ, $\dot{\rho}_i^L \neq \dot{\rho}_i^R$. Because $\dot{\eta}$ is continuous, this implies that every discontinuity in $\dot{\rho}$ is canceled either by discontinuity in $\dot{\mu}$ (camera tilt) or in $\dot{\Phi}$ (zoom transition).

First discontinuity to be identified is the zoom-transition at 13.5 s, marked in Fig. 3 as green triangle. The zoom-out starts at $t_{zo} = -0.2$ s, and is of known duration of $\Delta t_z = 13.7$ s, so it ends at the zoom-transition time of $t_{zT} = t_{zo} + \Delta t_z = 13.5$ s. However, toward the end of the first part of the video clip, it is obvious that past t_{zT} the camera is zooming-in. Obvious conclusion is that the zoom-out continued to 1:1 and then changed to zoom-in which continued to maximal value 6:1 that was reached at 27.2 s. This zooming behavior is listed in Tbl. I.

Then, the jump-discontinuity in $\dot{\rho}$ at $t = 13.5$ s has to be compensated by the jump-discontinuity in $\dot{\Phi}$, so

$$\frac{\dot{\rho}^L - \dot{\rho}^R}{\rho}(t^*) = \frac{\dot{\Phi}^R - \dot{\Phi}^L}{\Phi}(t^*). \quad (2.6)$$

Unfortunately, $\dot{\rho}$ is too noisy for this relationship to be useful in extracting $\dot{\Phi}$.

The discontinuities in $\dot{\mu}$ are most numerous and most easily identified from the video clip. At 2.1 s the camera starts to tilt upwards to follow the ascent, so $\dot{\mu}$ jumps from 0 to $+3^\circ/s$. Similarly, a sequence of four downwards tilts in which $\dot{\mu}$ jumps from 0 to $-3^\circ/s$ starting at 21.9 s is identified as such, because they keep the LM AS moving down in the camera FOV. So between 2.1 s and 21.9 s the camera had to stop tilting upwards, and the discontinuity at 20 s after liftoff is its obvious location.

This completes our discontinuity analysis of $\dot{\rho}$, and we summarize in Tbl. I. In Fig. 3 we show

functions η and ζ , and zoom and tilt regions of the camera (gray for camera tilting up, red for camera tilting down, no shade for camera not tilting, and green triangle that indicates transition from zoom-out to zoom-in).

Most importantly, the jump-discontinuities in $\dot{\rho}$ stemming from jumps in $\dot{\mu}$ at times t^* , allow us to deduce values of the zoom-function as,

$$\Phi(t^*) = \frac{\dot{\mu}^L - \dot{\mu}^R}{\dot{\rho}^R - \dot{\rho}^L}(t^*). \quad (2.7)$$

For better numerical accuracy in determining left and right slopes of $\dot{\rho}$, we can now use neighborhood around discontinuities. In Tbl. III we collect all so computed $\Phi^+(t^*)$ for $t^* \geq t_{ZT}$.

We assume that for the duration of zoom-in $t' = t - t_{ZT} \in [0, \Delta t_Z]$, the zoom-in function can be written as,

$$\Phi^+(t') = \frac{1 - q_1 t'}{1 + q_2 t'}, \quad (2.8)$$

with end-point values $\Phi^+(0) = 1$ and $\Phi^+(\Delta t_Z) = 1/6$. This zoom-function is consistent with a behavior of the focal point of a system of two lenses the distance between which changes at constant rate. As $\Delta t_Z = 13.7$ s is known from inspection of the video clip, and we know that zoom-in starts at t_{ZT} , we find through least-squares procedure that $q_1 = 0.0461 \text{ s}^{-1}$ and $q_2 = -6q_1 + 5/\Delta t_Z = 0.08833 \text{ s}^{-1}$. We show the best-fit line in Fig. 4 together with data from Tbl. III, and find an excellent agreement.

For computational convenience we also introduce zoom-out function $\Phi^-(t)$ as,

$$\Phi^-(t) = \frac{1 + \lambda_1 t}{6 - \lambda_2 t}, \quad (2.9)$$

where we find $\lambda_1 = 0.1250 \text{ s}^{-1}$ and $\lambda_2 = 0.2400 \text{ s}^{-1}$.

Time Start (s)	Time End (s)	Camera Motion	Tilt Rate ($^{\circ}/s$)	Description
-0.2	13.5	Zoom-Out		$\Phi^{-}(t + 0.2)$, Eq. (2.9)
13.5	27.2	Zoom-In		$\Phi^{+}(t - 13.5)$, Eq. (2.8)
2.1	20.0	Tilt Up	3	$\mu(t)$
20.0	21.9	No tilt	0	”
21.9	22.6	Tilt Down	-3	”
22.6	23.4	No tilt	0	”
23.4	24.4	Tilt Down	-3	”
24.4	25.1	No tilt	0	”
25.1	26.1	Tilt Down	-3	”
26.1	26.8	No tilt	0	”
26.8	27.8	Tilt Down	-3	”
27.8	28.2	No tilt	0	”

TABLE I: Discontinuities in $\dot{\rho}$ and their interpretation in terms of changes in the camera motion (tilt μ , and the direction of zoom Φ^{\pm}).

t (s)	$\mu(t)$ (deg)	Description
0.0	0.0	liftoff
2.1	0.0	tilt-up starts
20.0	53.7	tilt-up ends
21.9	53.7	tilt-down starts
22.6	51.6	tilt-down ends
23.4	51.6	tilt-down starts
24.4	48.6	tilt-down ends
25.1	48.6	tilt-down starts
26.1	45.6	tilt-down ends
26.8	45.6	tilt-down starts
27.8	42.6	tilt-down ends
30.0	42.6	

TABLE II: Linear interpolation table for the camera tilt, $\mu = \mu(t)$, in the absence of the initial offset of the camera, $\mu_0 = 0$.

t^* (s)	$\Phi^+(t^*)$
20.0	0.44
21.9	0.36
22.6	0.31
23.4	0.28
24.4	0.25
25.1	0.25
26.1	0.20
26.8	0.17
27.8	0.15

TABLE III: Zoom function Φ^+ is reconstructed from the magnitude of tilt discontinuities, and plotted in Fig. 4 with the best-fit model (2.8).

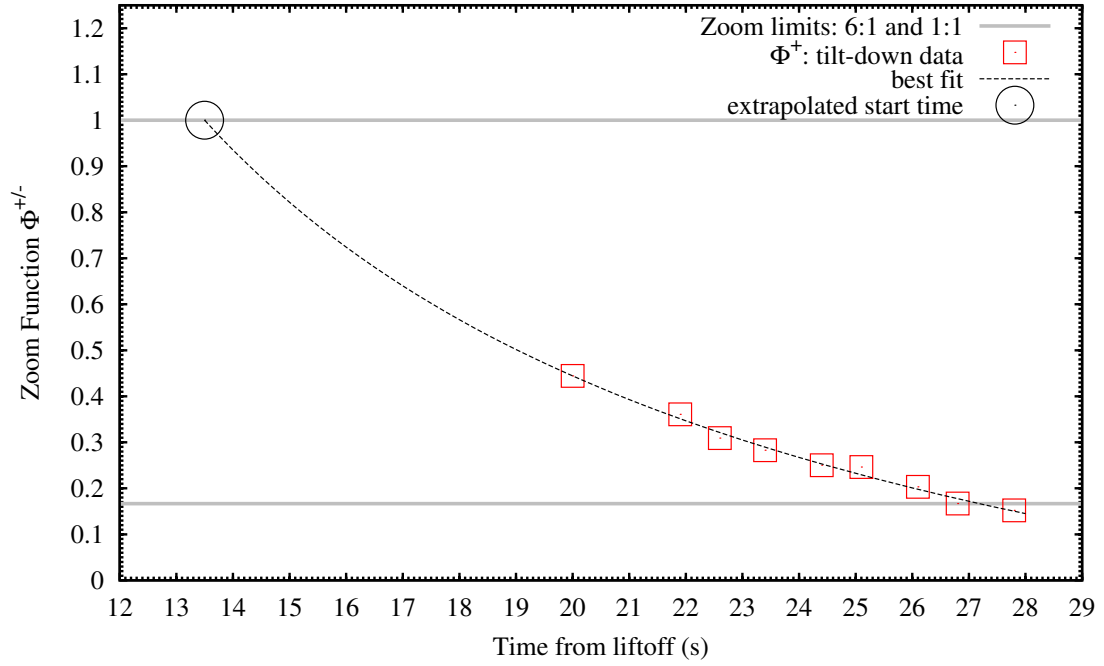


FIG. 4: Zoom function Φ^+ values from Tbl. III are nicely described with the best-fit model (2.8) from $t = 13.5$ s (zoom-out has reached 1:1 and switched to zoom-in) to 27.2 s (zoom-in has reached 6:1).

2.4. The Scene

For simplicity sake, we assume that the landing surface is approximately flat and that the camera vertical coincide with the landing surface vertical. From the frame -00:00.2 in [3] shown in Fig. 2, we extract the positions of all four landing feet. Then, from the offset of the front middle (Z-) foot from the midpoint between the Y- (left) and Y+ (right) feet, we find the angle

$$\gamma = 13.8^\circ, \quad (2.10)$$

between the line camera-LM AS, and the LM AS Z+ axis. Similarly, from the vertical angle between the feet Z- and Z+ we find that height of the camera above the launch site is

$$h_C = \frac{c^2}{\cos \gamma D} \cdot \Delta \phi = 7.2 \text{ m}, \quad (2.11)$$

where the diagonal distance between the feet is $D = 9.45 \text{ m}$ (=31 ft) and $\Delta \phi = 0.25^\circ$ is the vertical angle between the two feet at 6:1 zoom. For Eq. (2.11) we read the distance from the camera to the launch site from the map in Fig. 1,

$$c = 120 \text{ m}. \quad (2.12)$$

We re-evaluate this distance again in Sec. 5 in the Discussion.

Considering that the LM Descent Stage (DS) is $h_{DS} = 3.2 \text{ m}$ high, and that the AS is $h_{AS} = 2.8 \text{ m}$ high, we find that the the point B is at

$$x_0 \approx -h_C + h_{DS} = -4 \text{ m}, \quad (2.13)$$

that is, below the camera. As $x_0 = c \cdot \tan(\mu_0 + \Phi^-(-0.2)) \cdot \rho(-0.2)$, where $\rho(-0.2) = -8.7^\circ$ from Fig. 3, and $\Phi^-(-0.2) = 1/6$, we conclude that the camera vertical offset is,

$$\mu_0 = -0.45^\circ. \quad (2.14)$$

We combine μ_0 with the model from Eq.(2.2) and find the absolute elevation of the craft in the television broadcast [3] of the Apollo 17 ascent. This we report in Fig. 5 (black circles), and remark that this reconstruction is independent from the underlying motion of the craft.

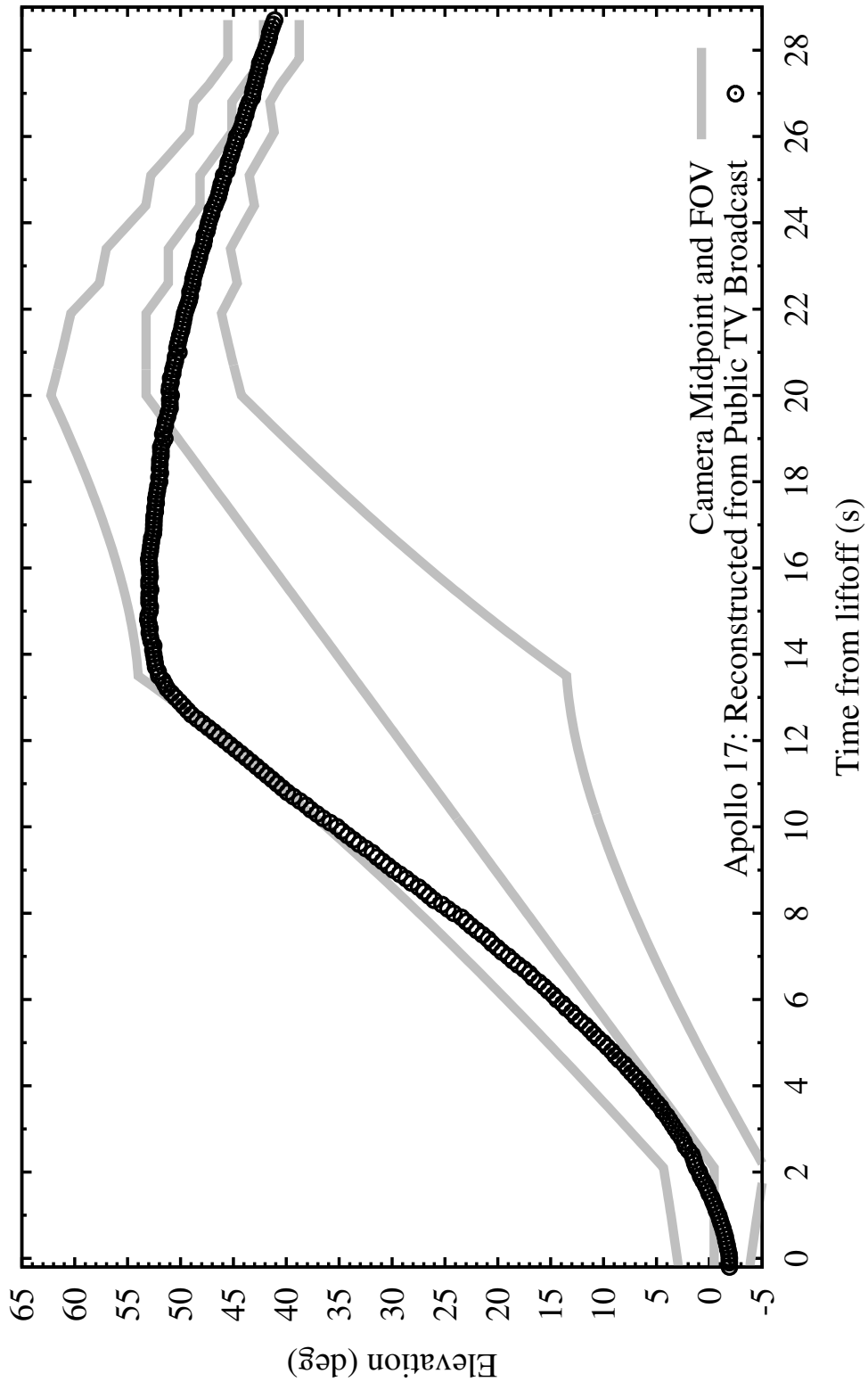


FIG. 5: The absolute elevation η of the craft in the television broadcast [3] of the Apollo 17 lunar ascent (black circles of approximate radius 1° to emphasize uncertainty) and the camera center and FOV (gray lines) as the functions of time.

3. THE APOLLO LUNAR ASCENT TRAJECTORY

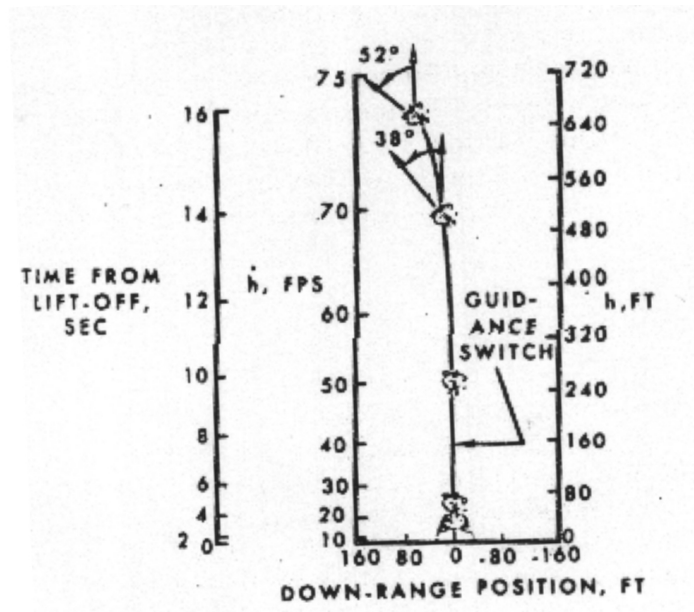


FIG. 6: The Vertical Rise Phase of the Apollo 11 LM AS. [12] Also shown is the nominal threshold for the guidance logic (digital autopilot) to switch to the Orbit Insertion phase.

The Lunar Module ascent from the surface was supposed to be the last part of the lunar stay of any Apollo mission. [12], The single objective of the ascent would be to achieve an orbit from which rendezvous with the orbiting Command and Service Module (CSM) could be executed. The target orbit was 16.7-by-44.4 km (9-by-24 nm) at a true anomaly of 18° , and the 18.3 km (=60,000 ft) altitude. The time of liftoff would be chosen so to provide the correct phasing for rendezvous. The target requirements were height, velocity, and orbit plane. Unlike the Descent Propulsion System (DPS), which featured a throttleable gimbal drive capable of adjustments of up to $\pm 6^\circ$, the Ascent Propulsion System (APS) would have a fixed gimbal angle and would not be throttleable (it would possess only “on” and “off” states). During the ascent the vessel would be steered by the guidance logic that controlled the Reactive Control System (RCS), so no input from the astronauts would be required. For that reason, the ascent would probably be quite similar, if not identical, between the Apollo missions.

With respect to the craft pitch θ from the vertical +X axis, the ascent comprised two phases, namely, the Vertical Rise (VR) phase, and the Orbit Insertion (OI) phase:

VR: Purpose of the Vertical Rise (VR) Phase was for the LM AS to achieve terrain clearance. During its first two seconds, which we refer to as the “Descent Stage Clear,” the guidance logic

would maintain the initial attitude (orientation) of the LM AS (with respect to the ambient). Then, the LM AS would adjust θ so that it flies straight up, and possibly rotate (yaw) so that in the end its XZ-plane would be parallel to the orbital plane of the CSM. The guidance logic would terminate the VR Phase after 10 s, or if the vertical velocity reached 15.3 m/s (=50 fps), whichever came first.

OI: The Orbit Insertion (OI) Phase would start with the guidance logic increasing the pitch θ in steps. In popular vernacular the first pitch change was referred to as the “pitch-over.” The OI Phase would terminate once the target orbit was reached in phase with the CSM.

3.1. Apollo 11 Data

The craft in the broadcast does not perform any yaw for the duration of recorded ascent. This suggests that the XZ plane of the craft on the ground must have been already parallel to the CSM orbit, cf. Fig. 2. In that XZ plane the motion of an LM AS is described by the rocket-motion equations,

$$\begin{aligned}\ddot{x} &= \tau_A \cos \theta - g, \\ \ddot{z} &= \tau_A \sin \theta,\end{aligned}\tag{3.1}$$

where τ is the thrust acceleration of the rocket, g is the local gravity, and $a = \tau_A - g$ is the resulting vertical acceleration of the rocket. Here the following comment is due. The thrust acceleration is, in fact, a function of time $\tau_A = \tau_A(t)$ because the total mass of the craft decreases by using the fuel for propulsion. More detailed analysis gives,

$$\tau_A(t) = \frac{\tau_A(0)}{1 - \frac{\dot{m}t}{m_0}},\tag{3.2}$$

where the propellant mass flow rate is $\dot{m} = 5.1$ kg/s, while the initial mass of the LM AS is $m_0 = 4,882$ kg. [13, 14] As for the short initial times t' , such that $\dot{m} \cdot t' \ll m_0$, the changes in mass can be neglected, we can assume $\tau_A(t) \simeq \tau_A(0)$ is a constant and drop its time dependency. As for the elevation $\eta = \eta(t)$ of the LM AS during the lunar ascent, this is given by,

$$\tan \eta = \frac{x}{\sqrt{c^2 + z^2 + 2cz \cos \gamma}} \approx \frac{x}{c + z \cos \gamma},\tag{3.3}$$

where the latter expression is valid for $|z| \ll c$, that is, for early OI.

Fig. 6 shows the VR and early OI Phases reported for the Apollo 11. [12] The vertical trajectory $x = x(t)$ is well described by a constant-acceleration motion starting from rest,

$$x(t) = \frac{a_{11}}{2} t^2, \quad (3.4)$$

where the liftoff occurs at $t = 0$. Here, the liftoff acceleration a_{11} was extracted from Fig. 6 to be,

$$a_{11} = 1.57 \text{ m} \cdot \text{s}^{-2} = \tau_{11} - g_M, \quad (3.5)$$

where the Moon gravity is $g_M = 1.62 \text{ m} \cdot \text{s}^{-2}$, while $\tau_{11} = 3.19 \text{ m} \cdot \text{s}^{-2}$ is the thrust acceleration of the Apollo 11 Ascent Propulsion System (APS) at liftoff.

The pitch-over occurred at $T_{VR} \simeq 10$ s (more precisely $15.2/1.57 = 9.7$) because the velocity threshold has been reached, and after some 14 s the LM AS was pitched by 38° . At 16 s from liftoff, the pitch was 52° . These pitch angles are consistent with the specifications of the Reactive Control System (RCS), which under the guidance logic (digital autopilot) would provide the pitch rates up to the maximal $10^\circ/\text{s}$. [15]

Based on this data we construct a linear interpolant for pitch angle $\theta = \theta(t)$ for Apollo-like lunar ascent in Tbl. IV. We remark that during the Vertical Rise and Early Orbit Insertion the pitch cannot be above the maximal value $\theta_{max} \simeq 52^\circ$, because this assures that the craft continues to accelerate upwards, $\ddot{x} = \tau \cos \theta - g_M \geq 0$.

time	$\theta(t)$	Comment
0.0	0°	Descent Stage Clear / Vertical Rise
T_{VR}	0°	“Pitch-over”
$T_{VR}+6$ s	52°	End of continuous coverage in TV broadcast
30 s	52°	

TABLE IV: Linear interpolant table for the pitch angle in an Apollo-like lunar ascent, assuming that the duration of the Vertical Rise is some T_{VR} , not necessarily 10 s as was the case with the Apollo 11.

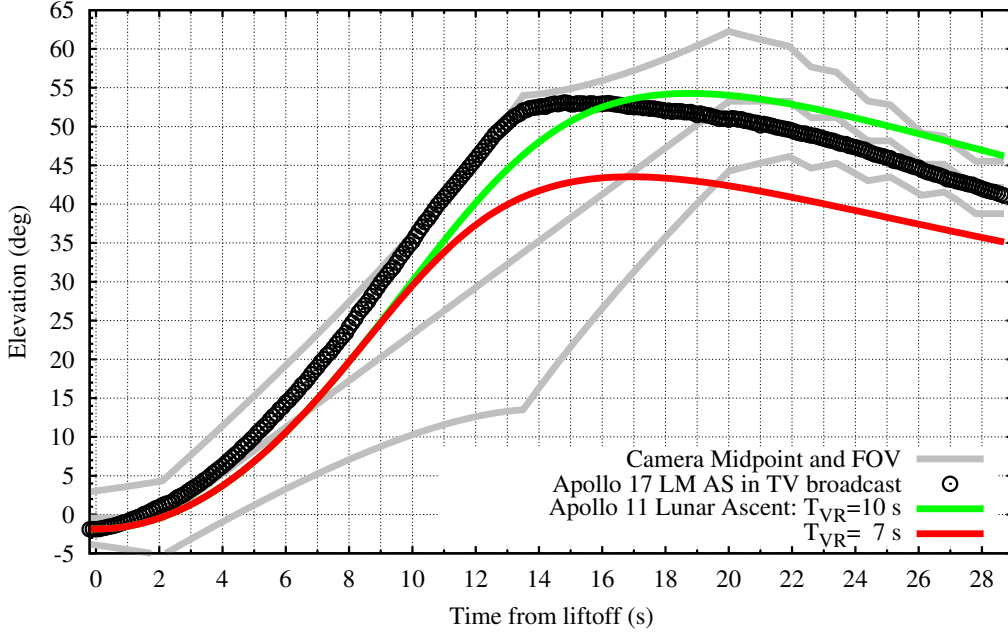


FIG. 7: The motion of the craft from the Apollo 17 television broadcast [3] of lunar ascent does not match the Apollo 11 ascent trajectories either with the reported $T_{VR} = 10$ s or with the hypothetical $T_{VR} = 7$ s. The schedule for $\theta = \theta(t)$ is provided in Tbl. IV.

4. VERTICAL RISE AND EARLY ORBIT INSERTION PHASE OF THE CRAFT IN TV BROADCAST

It is difficult to determine from the inspection of the television broadcast [3] when the craft started turning. However, in the frame 00:11.5 the viewer can get clear view of the bottom of the craft. At that time the craft elevation is $\eta(11.5 \text{ s}) \approx 45^\circ$, so the pitch is

$$\theta(11.5 \text{ s}) = 90^\circ - \eta(11.5 \text{ s}) \approx 45^\circ. \quad (4.1)$$

Considering that the maximal turning rate of the guidance logic (digital autopilot) is $\dot{\theta} = 10^\circ/\text{s}$, this suggests that the Vertical Rise ended not later than

$$T_{VR} \leq 11.5 - 45/10 \simeq 7 \text{ s}. \quad (4.2)$$

This we investigate further by introducing the projected vertical position $\hat{x} = \hat{x}(t)$ of the craft in television broadcast [3], given by

$$\hat{x}(t) = c \cdot \tan \eta(t), \quad (4.3)$$

with c the distance between the camera and the launch site given in Eq. (2.12) sourced from the map in Fig. 1.

The second degree polynomial,

$$P_2(t; a, v_0, x_0) = \frac{a}{2}t^2 + v_0t + x_0, \quad (4.4)$$

is an excellent description for $\hat{x}(t)$ for $t \in [0, T_{VR}]$. We find its terms by minimizing the Mean-Root Square Error (MSRE),

$$\text{MSRE}^2(T_{VR}) = \frac{1}{N-3} \sum_{i=1}^N (\hat{x}_i - P_2(t_i; a, v_0, x_0))^2, \quad (4.5)$$

where $\hat{x}_i = \hat{x}(t_i)$, while $N = N(T_{VR})$ is the number of points in the data set $t_i \in [0, T_{VR}]$. We show minimum of the MSRE in Fig. 8 for T_{VR} in the range 6 to 10 s (top panel). In parallel, we introduce difference $\Delta x = \Delta x(t)$, as

$$\Delta x(t) = \hat{x}(t) - P_2(t; \hat{a}, \hat{v}_0, \hat{x}_0), \quad (4.6)$$

where the best-fit parameters

$$\begin{aligned} \hat{a} &= 1.45 \pm 0.06 \text{ m} \cdot \text{s}^{-2}, \\ \hat{v}_0 &= 1.4 \pm 0.2 \text{ m} \cdot \text{s}^{-1}, \\ \hat{x}_0 &= -3.9 \pm 0.4 \text{ m}, \end{aligned} \quad (4.7)$$

are calculated for the same $T_{VR} = 7$ s. In the bottom panel of Fig. 8 we show the B-spline smoothed Δx from Eq. (4.6) in red. That the value $T_{VR} = 7$ s is self-consistent follows from the fact that the first derivative does not change its sign, $d\Delta x/dt \geq 0$ for $t \geq T_{VR}$. More importantly, the behavior of $\Delta x(t)$ for the craft in television broadcast [3] is such that its vertical acceleration increases for some time after the pitch-over.

We compare the craft Δx to that of a hypothetical LM AS powered by the Apollo APS. This we do by solving Eq. (3.1) using the Apollo 11 thrust acceleration and pitch schedule from Tbl. IV, and \hat{x}_0 from Eq. (4.7). The behavior of $\Delta x(t)$ for the nominal Apollo APS is as expected: After the pitch-over the Apollo LM AS vertical acceleration decreases.

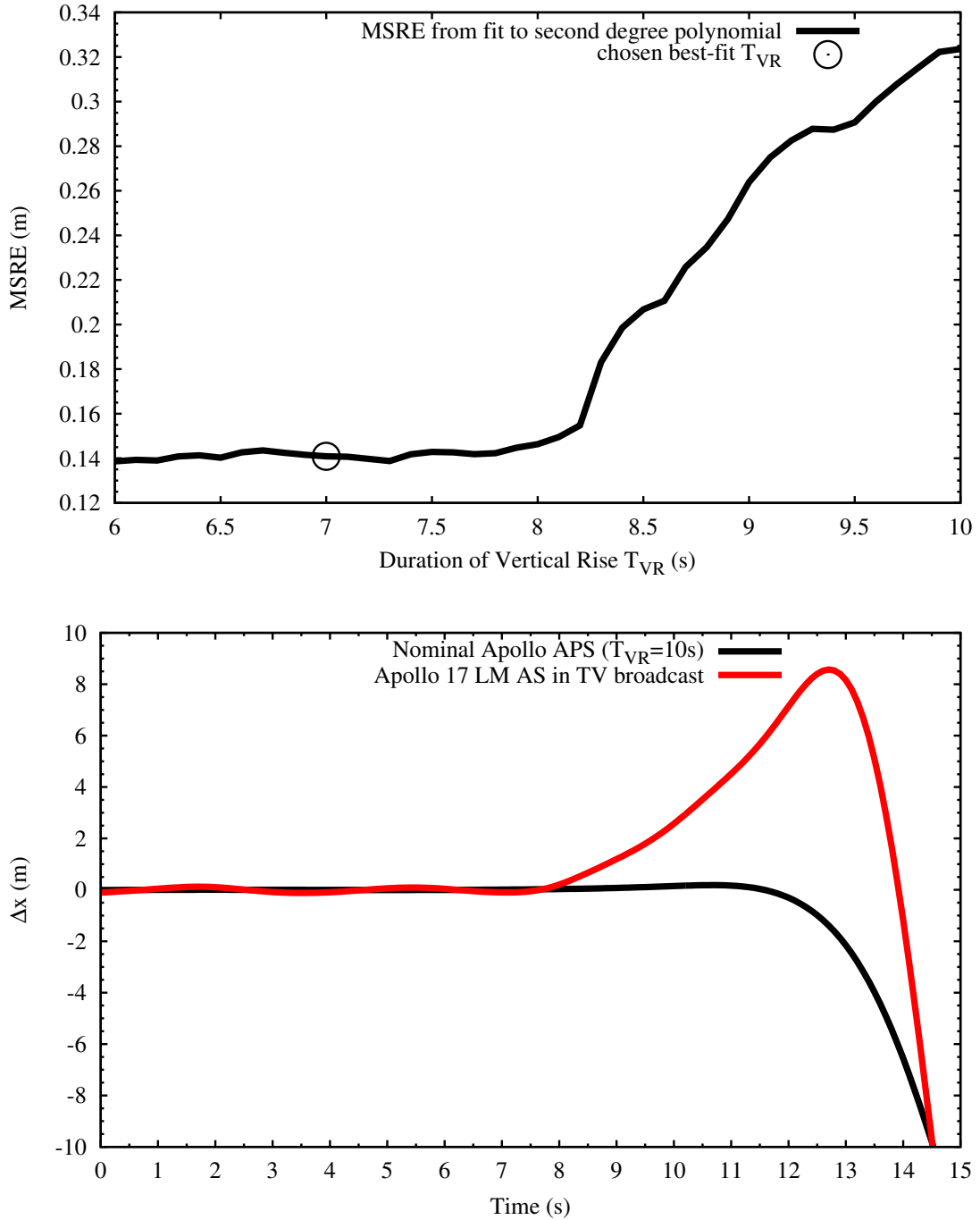


FIG. 8: (Top Panel) MSRE (4.5) as a function of T_{VR} (top panel) suggests that the Vertical Rise of the craft in the television broadcast [3] lasted 7 seconds. (Bottom panel) Behavior of $\Delta x = \Delta x(t)$, Eq. (4.6), and its first derivative is consistent with $T_{VR} = 7$ s. More importantly, Δx of the nominal Apollo APS ascent trajectory (black line) significantly differs from that of the craft in the television broadcast [3] (red line): the acceleration of the craft increases as it turns away from the vertical.

5. DISCUSSION AND CONCLUSIONS

From the analysis of the Vertical Rise and the Early Orbit Insertion Phases we have found the following discrepancies in the performance between the nominal Apollo Lunar Module (LM) Ascent Stage (AS) and its Ascent Propulsion System (APS), and the craft in the television broadcast [3]:

1. Ed Fendell story

It is known that the delay between the start of the Apollo APS and the liftoff was fixed between 0.2 and 0.3 s. This we say because the camera started to zoom-out the same amount of time before the liftoff of the craft. Thus it is not inconceivable that at the launch site, as the engine was started the camera began executing received commands. On the other hand, the NASA camera operator Ed did not actually look at the live feed when he was commanding the camera. Rather he stated, he prepared the commands beforehand and then sent them based on the timer synchronized to the launch schedule. For this to work he had to know what was the round-trip travel time of the communication signal. In [16] he said this was three seconds, while in [17] he was quoted saying that was two seconds. In the absence of official NASA value, among Apollo enthusiasts this was circulated to be 1.3 s. Thus, a command sent at three second mark would reach the launch site at $-3 - 0.3 + 2 \cdot 1.3 = -0.7$ s (before the liftoff), while a command sent at two second mark would be at the launch site 0.3 s after the liftoff. Adding two human response times of 0.1 s (one for commander announcing, the other for Ed reacting) does not resolve this. However, the problem with any of this is that the only time mark announced by the crew occurred at 188:01:27 GET at 10 s mark [18]. Interestingly the uplink from LM to ground control was lost around that time and would not be regained for the next four minutes.

In the same sources [16, 17] Ed stated that he communicated to the commander how far the camera should be from the launch site. In official record of all oral communication between the ground control and the crew, the Apollo Lunar Flight and Surface Journal, no such communication is ever reported. In fact, on their web site two different values (for what we labeled c) are listed, $c' = 158$ m at [19], and $c'' = 145$ m at [20]. Using either of these distances instead of $c = 120$ m from Eq. (2.12) means that the values from Eq. (4.7) have to be multiplied by $c'(\prime\prime)/c$ instead. As $c'(\prime\prime)$ is 21% (32%) greater than c these results in accelerations that exceed those reachable by the Apollo APS. [25] In other words, were

the distance to the launch site exceeding c then the craft in the television broadcast [3] is definitely not an Apollo LM ascent stage.

2. The craft overall ascent trajectory is not similar to the nominal Apollo APS trajectories with either $T_{VR} = 10$ s or 7 s, cf. Fig. 7.
3. The craft begins pitch-over too early at $T_{VR} \simeq 7$ s.

It is not clear what triggered the guidance logic (digital autopilot) to start to change the pitch θ : From the best-fit parameters of the craft motion, at the end of the Vertical Rise the craft velocity is

$$v(T_{VR}) = \hat{a}T_{VR} + \hat{v}_0 \simeq 11.5 \text{ m} \cdot \text{s}^{-1} = 38 \text{ fps}, \quad (5.1)$$

which is below the $15.2 \text{ m} \cdot \text{s}^{-1}$ (=50 fps) velocity threshold, and 10 s has not yet expired.

4. The craft's initial velocity $v_0 = 1.4 \text{ m} \cdot \text{s}^{-1}$ is too great.

This fact has been discussed on the internet forums since Braeunig published simulation of the Apollo 17 liftoff based on zero initial velocity [21]. To our knowledge there are two explanations for this phenomenon that are being circulated among Apollo enthusiasts. First is that this was some sort of transient associated with the starting of the APS rocket engine, while the second is that this was caused by, so called, "Fire in the Hole" effect. [22]

As we show next, neither of these explanations survives quantitative scrutiny.

In [23] (cf. Fig. 8 therein) the initial transients of an APS rocket engine were captured. These transients can be approximately described as peaking at ignition time at f_{pk} and then linearly decaying to 0 over the transient duration time t_{tr} . This type of transient creates an initial velocity v_{tr} , given by

$$v_{tr} \approx \frac{1}{2} f_{pk} t_{tr}. \quad (5.2)$$

The analysis reported $f_{pk} \simeq 0.5 \cdot \tau \sim 1.5 \text{ m} \cdot \text{s}^{-2}$, with $t_{tr} \simeq 100$ ms. Following Eq. (5.2) this contributes with $v_{tr} \sim 0.25 t_{tr} \tau \sim 0.1 \text{ m} \cdot \text{s}^{-1}$, which is too little compared to the observed $v_0 = 1.4 \text{ m} \cdot \text{s}^{-1}$, that is, $v_{tr} \ll v_0$.

Similarly, non-zero v_0 is neither caused by the, so called, "Fire-in-the-Hole" effect: It has been quickly recognized that firing a rocket engine against a flat surface close by, may introduce additional (destabilizing) forces on the craft, due to effective accumulation of the exhaust gases between the craft and the surface. The study of the effect was one of the

important goals of the Apollo 5 mission [24] early in the space program. However, no v_0 has ever been reported either for the Apollo 5 LM AS separation from the Descent Stage, or for the lunar ascent of the Apollo 11 mission, meaning, $v_0 \approx 0$ always.

To estimate the magnitude of the actual transient that produced $v_0 \gtrsim 1 \text{ m}\cdot\text{s}^{-1}$, we may assume that its duration was $t_{tr} \sim 0.1 - 0.2 \text{ s}$, yielding the peak acceleration $f'_{pk} \simeq 2v_{tr}/t_{tr} \simeq 28$ down to $14 \text{ m}\cdot\text{s}^{-2}$. Such f'_{pk} is some 5 to 10 times greater than the thrust acceleration $\tau_{17} \sim 3.1 \text{ m}\cdot\text{s}^{-2}$ of the Apollo APS could provide for the lunar ascent. We foresee two alternative explanations, where by the first an explosion took place underneath the LM AS, and by the second the actual thrust acceleration of the rocket engine of the craft was much smaller than what the TV broadcast had let us believe. As for the former, besides not being corroborated by the mission documents, the TV broadcast does not support it either. Consider that the same force that accelerated the LM AS also acted on the spent Descent Stage (DS). The magnitude of this force may have been as high as $F' = m_0 \cdot f'_{pk} \sim 120 \text{ kN}$ and was acting upon the DS in highly asymmetric fashion. Considering that single landing gear could stand 20 kN before flexing, in response to F' the DS would have to be visibly perturbed. However, in the TV broadcast the DS and its landing gears do not move a single pixel in response to the lift-off. We are thus left with the latter hypothesis, that the thrust accelerations and the lift-off forces were much smaller in magnitude than they appeared to have been.

5. The craft jerks forward as it turns away from the vertical.

As shown in Fig. 8 bottom panel (in black), during the ascent from lunar surface the vertical acceleration would have decreased as the LM AS turned away from the vertical.. The acceleration of the craft in the television broadcast [3] (in red), on the other hand, increased for some time after it turned away from the vertical. This forward jerk is not consistent with a free flying rocket in space.

In conclusion, the lunar ascent of the craft in the television broadcast [3] is in some important aspects different from what one would expect of an Apollo-like APS and its guidance logic (digital autopilot), flying freely (or unconstrained) in space. The constraints on the motion of a rocket that produce the effects reported above and their scale can be extracted, nonetheless. These constraints and their scale are subject of a current study and they will be reported elsewhere.

Conflict of interest statement: The author states that there is no conflict of interest.

- [1] NASA, in *Apollo 17 Traverse Planning Data, 3rd Edition* (1972), Fig. 23 on p. 97, [Online; accessed January 18, 2014], URL <https://www.hq.nasa.gov/alsj/a17/A17TraversePlanningData.pdf>.
- [2] Apollo Lunar Surface Journal, *Apollo 17 Mission Overview* (1996-2013), [Online; accessed April 12, 2015], URL <http://www.hq.nasa.gov/alsj/a17/a17ov.html>.
- [3] YouTube.com, *Apollo 17 Lunar Liftoff*, [Online; accessed June 25, 2014] At that time the video clips were downloaded locally in flash format, and these copies are available upon request. Recently we have learnt that some of the links are no longer valid, URL <https://www.youtube.com/watch?v=g9Zys0Bs4UU>, <https://www.youtube.com/watch?v=Dr98RgNjAgg>, <https://www.youtube.com/watch?v=XlGis35Epvs>.
- [4] W.F. Schreiber, *Proceedings of the IEEE* **87** (1999).
- [5] Ken Glover, *Apollo Lunar Surface Journal* (1996-2013), [Online; accessed January 21, 2014] published originally as NASA Technical Note TN-A7476, URL <http://www.hq.nasa.gov/alsj/LC-SOW.pdf>.
- [6] Radio Corporation of America, *NASA-CR-128829 - Ground-Commanded Television Assembly (GCTA) - Interim Final Report* (31. July 1970 - 15 February 1972), [Online; accessed January 18, 2014], URL <http://ntrs.nasa.gov/archive/nasa/casi.ntrs.nasa.gov/19730010465.pdf>.
- [7] The FFmpeg developers, *FFmpeg 2.6.1* (2015), <https://www.ffmpeg.org>.
- [8] NASA, in *Apollo 17 Press Kit* (1972), p. 78, URL https://www.hq.nasa.gov/alsj/a17/A17_PressKit.pdf.
- [9] L. Ma, C. Cao, A. Young, and N. Hovakimyan, in *AIAA Guidance, Navigation and Control Conference and Exhibit* (Honolulu, Hawaii, USA, August 18-21, 2008).
- [10] O. Faugeras, *Three-dimensional Computer Vision: A Geometric Approach* (MIT Press, 1996), pp. 138.
- [11] Zeiss, *Biogon f/5.6-60mm Lens for Hasselblad-C cameras*, URL <https://www.zeiss.com/content/dam/camera-lenses/files/service/download-center/datasheets/historical-lenses/hasselblad-c/datasheet-zeiss-biogon-5660-en.pdf>.
- [12] NASA, *Technical Memorandum TM X-58040 Apollo Lunar Descent and Ascent Trajectories* (March, 1970), URL <https://www.hq.nasa.gov/alsj/nasa58040.pdf>.

- [13] Grumman, *Apollo News Reference - Lunar Module Quick Reference Data*, [Online; accessed June 25, 2015], URL https://www.hq.nasa.gov/alsj/LM04_Lunar_Module_ppLV1-17.pdf.
- [14] NASA, *Apollo Operations Handbook - Lunar Module LM 10 and Subsequent Subsystems Data - Volume I* (1970), [Online; accessed January 18, 2014], URL <https://www.hq.nasa.gov/alsj/alsj-LMdocs.html>.
- [15] Robert F. Stengel, J. Spacecraft and Rockets **7**, 941 (1970), Presented as Paper 69-892 at the AIAA Guidance, Control and Flight Mechanics Conference, Princeton, NJ, August 18-20, 1970.
- [16] NASA Johnson Space Center, Oral History Project, *Edward I. Fendell, interviewed by Kevin M. Rusnak* (19 October 2000), URL https://www.jsc.nasa.gov/history/oral_histories/FendellEI/FendellEI_10-19-00.htm.
- [17] R. Houston and M. Heflin, *Go, Flight! The Unsung Heroes of Mission Control, 1965-1992* (University of Nebraska Press, December 2015), p. 278. Preview available on GoogleBooks.
- [18] Eric M. Jones, *Apollo 17 Lunar Surface Journal - Return to Orbit* (1995. Last revised 17 June 2014), [Online; accessed June 13, 2017], URL <https://www.hq.nasa.gov/office/pao/History/alsj/a17/a17.launch.html>.
- [19] Eric M. Jones, *Apollo Lunar Surface Journal - Final LRV Parking Places* (Last revised 25 October 2005), [Online; accessed June 13, 2017], URL <https://www.hq.nasa.gov/alsj/alsj-LRVFinalParking.html>.
- [20] Eric M. Jones, *Apollo 17 Multimedia - Video Library* (Last revised 15 August 2011), [Online; accessed June 13, 2017], URL <https://www.hq.nasa.gov/alsj/a17/video17.html#closeout3>.
- [21] Robert A. Braeunig, (*Apollo 17*) *Lunar Module Ascent Simulation* (2009), [Online; accessed April 11, 2010], URL <http://www.braeunig.us/apollo/LM-ascent.htm>.
- [22] ApolloHoax.net Forum, *Topic: Apollo 17 ascent module liftoff*, [Online; accessed July 3, 2017], URL <https://www.apollohoax.net/forum/index.php?topic=655.30>.
- [23] J. C. Melcher IV and J. K. Allred, in *45th AIAA/ASME/ASEE Joint Propulsion Conference and Exhibit* (Denver, Colorado, USA, August 2-5, 2009).
- [24] NASA, *Apollo 5 Mission Report* (March, 1968), URL https://archive.org/download/nasa_techdoc_19800074521/19800074521.pdf.
- [25] To our knowledge the LM AS maximal acceleration was $a = \tau_5 - g_M = 1.71 \text{ m}\cdot\text{s}^{-2}$, where $\tau_5 = 3.33 \text{ m}\cdot\text{s}^{-2}$ was recorded in the Apollo 5 mission, cf. [24], Fig. 6.10-12 on p. 6.10-24. This was automated test flight in low-Earth orbit.